EUROPEAN TRANSACTIONS ON TELECOMMUNICATIONS
Eur. Trans. Telecomms. 2008; **19**:561–569
Published online 2 June 2008 in Wiley InterScience
(www.interscience.wiley.com) DOI: 10.1002/ett.1304

Analysis and design of OFDM-IDMA systems‡

Jun Tong, Qinghua Guo and Li Ping*

Department of Electronic Engineering, City University of Hong Kong, Kowloon, Hong Kong SAR, P.R. China

SUMMARY

This paper deals with the analysis and design of orthogonal frequency-division multiplexing interleave-division multiple-access (OFDM-IDMA). We begin with the analysis of the information-theoretical advantages of non-orthogonal transmission schemes in fading multiple-access channels. We then turn attention to practical design issues. A signal-to-noise ratio (SNR) evolution technique is developed to predict the bit-error-rate (BER) performance of OFDM-IDMA. This technique is applied to system design and optimisation. Through proper power allocation, OFDM-IDMA can achieve the multi-user gain (MUG) predicted by information-theoretical analysis. It is also an attractive option in compensating for the clipping effect caused by peak-power limitation. Numerical examples show that OFDM-IDMA can (i) alleviate the PAPR problem commonly suffered by OFDM-based schemes; (ii) deliver significant MUG compared with other orthogonal alternatives; (iii) provide robust communications in frequency-selective channels; and (iv) support high single-user throughput. Copyright © 2008 John Wiley & Sons, Ltd.

1. INTRODUCTION

Multiple-access interference (MAI) and inter-symbol interference (ISI) are major sources of impairments in wireless communication systems. Conventional multi-user detection (MUD) and time-domain equalisation techniques are very costly. However, it has been shown recently that these two types of interference can be efficiently resolved by using an orthogonal frequency-division multiplexing interleave-division multiple-access (OFDM-IDMA) scheme [1–3]. In OFDM-IDMA, ISI is treated by the cyclic prefixing technique in OFDM [4], and MAI by iterative detection with IDMA [5]. Compared with conventional multi-carrier schemes, OFDM-IDMA has several noticeable advantages such as low-cost receiver, diversity against fading and flexible rate adaptation.

This paper is concerned with the analysis and design techniques for OFDM-IDMA. First, we investigate the information-theoretical advantages of non-orthogonal transmissions in fading multiple-access channels. We show that non-orthogonal schemes can achieve significant performance improvement over orthogonal schemes. Such improvement is refereed to as 'multi-user gain (MUG)' because it is only achievable through MUD. This provides a motivation for optimising the performance of OFDM-IDMA systems according to theoretical prediction.

We then turn attention to some practical issues. We will outline a signal-to-noise ratio (SNR) evolution technique to analyse the performance of OFDM-IDMA, with which, the bit-error-rate (BER) performance of OFDM-IDMA can be quickly predicted. We will apply this technique to system design and optimisation. We will explain following noticeable advantages for OFDM-IDMA: first, a clipping technique can be used in OFDM-IDMA to reduce the peak-to-average power ratio (PAPR), which resolves a common problem for OFDM-based schemes [6, 7]. Second, power allocation can be applied to deliver the MUG promised by theoretical analysis. Third, OFDM-IDMA is robust against frequency-selective fading when low-rate coding is used to provide diversity gain. Finally, a superposition coding technique [8] can be applied to maintain high throughput. Numerical examples are provided to confirm these properties.

* Correspondence to: Li Ping, Department of Electronic Engineering, City University of Hong Kong, Kowloon, Hong Kong SAR, P.R. China.
E-mail: eeliping@cityu.edu.hk
‡ A previous edition of the paper has been presented in the 6th International Workshop on Multi-Carrier Spread Spectrum (MC-SS 2007).

Copyright © 2008 John Wiley & Sons, Ltd.
Accepted 6 May 2008

2. MOTIVATION

Before going into the details, we first provide in this section a compelling motivation for the introduction of non-orthogonal transmission in fading environments. We focus on the minimum transmitted-sum-power (MTSP) to support reliable communications. We will show that non-orthogonal options can significantly outperform orthogonal ones with regard to MTSP. This advantage is referred to as MUG because it is achievable only through MUD.

Consider a K-user multiple-access system over quasi-static flat-fading channels. We assume that the channel gains $\{h_k\}$ are independent, identically distributed (i.i.d.) and perfectly known at the transmitters and receiver. For simplicity, suppose that the system sum rate is R bits/s/Hz and the rate of each user is R/K.

Let the received signal in a multiple-access channel be written as

$$y = \sum_{k=1}^{K} h_k x_k + n \tag{1}$$

where x_k is user-k's transmit signal and n is an additive white Gaussian noise (AWGN) with variance N_0. We assume that $\{x_k\}$ are independent, Gaussian distributed.

We first consider the AWGN channel (i.e. $h_k = 1, \forall k$). Suppose that the successive interference cancelation (SIC) strategy [9] is applied at the receiver. We will use the descending decoding order indexed on k with x_K decoded first and x_1 last. Denote by q_k the received power for user k. From information theory [9], the minimum received power for user-k with SIC is given by

$$q_k = \left(2^{\frac{R}{K}} - 1\right)\left(N_0 + \sum_{i=1}^{k-1} q_i\right) = N_0\left(2^{\frac{R}{K}} - 1\right)2^{\frac{R(k-1)}{K}} \tag{2}$$

Now consider a flat-fading channel with fixed $\{h_k\}$. We control the transmit power of user-k to

$$p_k^{\text{optimal}} = \frac{q_k}{|h_k|^2} = \frac{N_0\left(2^{(R/K)} - 1\right)2^{(R(k-1)/K)}}{|h_k|^2} \tag{3}$$

so as to maintain the same received power profile $\{q_k\}$ as that in Equation (2) for the AWGN channel. Given $\{|h_k|^2\}$, a permutation of $\{|h_k|^2\}$ can be obtained by re-indexing its elements. For example, $\{|h_1|^2 = 1, |h_2|^2 = 2\}$ is a permutation of $\{|h_1|^2 = 2, |h_2|^2 = 1\}$. According to Reference [9], among all possible permutes of $\{|h_k|^2\}$, the minimum of the following sum of transmit powers

$$\sum_{k=1}^{K} p_k^{\text{optimal}} = N_0\left(2^{(R/K)} - 1\right)\sum_{k=1}^{K}\frac{2^{(R(k-1)/K)}}{|h_k|^2} \tag{4}$$

is achieved when

$$|h_1|^2 \leqslant |h_2|^2 \leqslant \cdots \leqslant |h_K|^2 \tag{5}$$

where Equation (5) is referred to as the optimal decoding order. It can be shown that in this case, Equation (4) gives the theoretical limit of MTSP. It is interesting to compare Equation (4) with the result of an orthogonal strategy in which the signals from the K users are orthogonal to each other and they equally share the channel resources. Let the (long-term average) rate per user be R/K (so sum rate $= R$) and, according to channel capacity formula, the minimum transmit power is

$$p_k^{\text{orthogonal}} = \frac{N_0\left(2^R - 1\right)}{K|h_k|^2} \tag{6}$$

For example, consider TDMA. Let the instantaneous rate be R in the active time slot for a user and so the long-term average rate is R/K per user. In this case, the minimum instantaneous transmit power is $N_0(2^R - 1)/|h_k|^2$ in the active time slot for a user and its average over K slots is given in Equation (6). It can be shown that Equation (6) holds for other orthogonal schemes. Based on Equation (6), the MTSP for an orthogonal scheme is

$$\sum_{k=1}^{K} p_k^{\text{orthogonal}} = \frac{N_0(2^R - 1)}{K}\sum_{k=1}^{K}\frac{1}{|h_k|^2} \tag{7}$$

MUG refers to the difference between Equations (4) (with optimal decoding order) and (7). Intuitively, such an advantage is achieved by matching the elements of two sets $\{|h_k|^2\}$ and $\{q_k\}$ in a large-to-large/small-to-small manner. Such ordered matching is possible only in a non-orthogonal environment. There is no MUG in an AWGN channel where $|h_k|^2 = 1, \forall k$. Hence, MUG comes from the near–far effect in fading channels together with the matching strategy. Due to the non-orthogonal nature, MUD is necessary at the receiver for optimal detection.

The above discussions assume fixed channel gains $\{|h_k|^2\}$. Practical $\{|h_k|^2\}$ are random variables. Therefore, we are interested in the MTSP averaged over the distribution of $\{|h_k|^2\}$. Figure 1 shows average MTSP *versus* R for different multiple access schemes over flat-fading

Copyright © 2008 John Wiley & Sons, Ltd.

DOI: 10.1002/ett

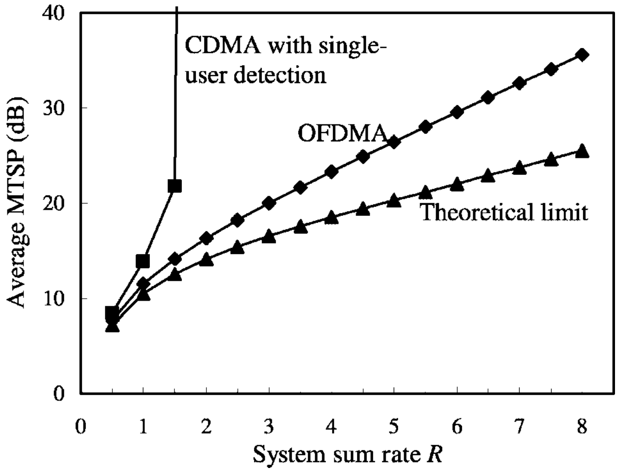

Figure 1. Average MTSP *versus* system sum rate R for different multiple-access schemes. $K = 4$ users are uniformly distributed in a hexagon cell. The channel effect includes path loss (the fourth law), lognormal fading (standard deviation = 8 dB) and Rayleigh fading. The distance from the farthest corner of the cell to the base station is 1. The lognormal fading is scaled such that its mean equals 1. The outage probability is 1 per cent.

channels, where orthogonal frequency-division multiple-access (OFDMA) is used as a representative orthogonal scheme. We can see that there is a significant gap (i.e. MUG) between the theoretical limit and the OFDMA performance. This gap increases with K.

Note that the theoretical limit can only be achieved by non-orthogonal transmission schemes with MUD [9]. Without MUD, performance degrades significantly, as seen from the curves in Figure 1 labelled as 'CDMA with single-user detection'. Only flat fading is considered in Figure 1. In the case of frequency-selective fading, OFDMA performance can be improved by water-filling while theoretical limit can be achieved by multi-user water-filling over a non-orthogonal scheme. The trend is similar to that shown in Figure 1, so the details are omitted.

From Figure 1, MUG becomes significant when rate increases. This provides the motivation for the OFDM-IDMA scheme presented below, in which the orthogonality of OFDM is employed in suppressing ISI while the non-orthogonality of IDMA is explored in realising MUG. The overall system is non-orthogonal.

3. TRANSMITTER PRINCIPLES

A K-user OFDM-IDMA system is illustrated in Figure 2. The system structure follows the principles proposed in Reference [1]. For user-k, the information data are forward-error-correction (FEC)-encoded into $\boldsymbol{c}_k = \{c_k[m]\}$. The sequence $\boldsymbol{c}_k$ is interleaved by a user-specific interleaver π_k and then mapped to a complex vector $\boldsymbol{x}_k = [x_k[0], \cdots, x_k[N-1]]^T$ using quadrature phase-shift keying (QPSK), where N is the number of sub-carriers and '$(\cdot)^T$' denotes matrix transpose. Each dimension of $x_k[n]$ (denoted by $x_k^{\mathrm{Re}}[n]$ or $x_k^{\mathrm{Im}}[n]$) represents a bit in $\boldsymbol{c}_k$. Then $\{x_k[n]\}$ are modulated onto sub-carriers using the inverse discrete Fourier transform (IDFT). The resultant signal is over-sampled into $\boldsymbol{X}_k = [X_k[0], \cdots, X_k[QN-1]]^T$, where Q is the over-sampling factor and $X_k[i] = 1/\sqrt{N}\sum_{n=0}^{N-1} x_k[n]\mathrm{e}^{j\frac{2\pi in}{QN}}$ with $j = \sqrt{-1}$.

Due to the IDFT operation, the time-domain signal is a weighted sum of N QPSK symbols, which has a high PAPR. We adopt a straightforward remedy by clipping to suppress the PAPR. The clipped signal is given by:

$$\mathrm{clp}(X_k[i]) = \begin{cases} X_k[i], & |X_k[i]| < A \\ AX_k[i]/|X_k[i]|, & |X_k[i]| \geqslant A \end{cases} \tag{8}$$

where $|\cdot|$ denotes amplitude and $A > 0$ is the clipping threshold. Then, $\{\mathrm{clp}(X_k[i])\}$ are band-pass filtered and

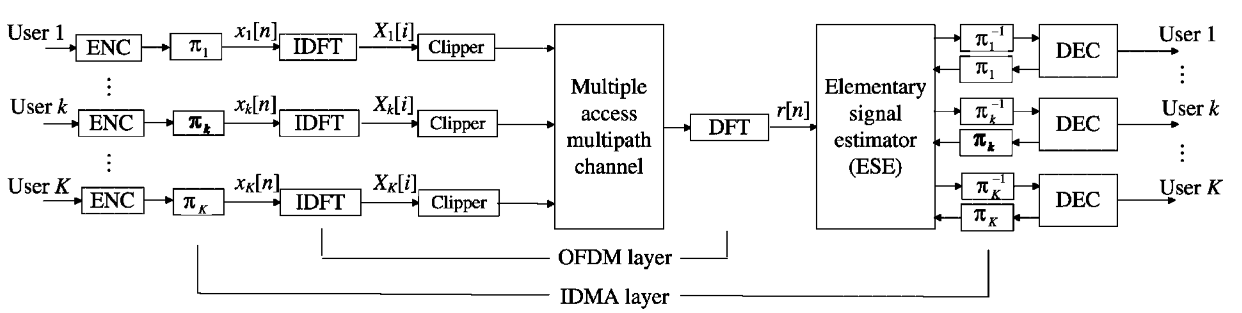

Figure 2. Transmitter/receiver structure for OFDM-IDMA. The QPSK modulation, cyclic prefix insertion and removal for OFDM are not shown for simplicity. ENC and DEC denote encoder and decoder, respectively.

Copyright © 2008 John Wiley & Sons, Ltd.

transmitted.[†] The clipping ratio (in decibel) is defined as $\mathrm{CR} = 10\log_{10}(A^2/\mathrm{E}[|X_k[i]|^2])$, where $\mathrm{E}[\cdot]$ denotes the mathematical expectation.

Note that the clipping operation in Equation (8) is nonlinear. Following Reference [7], we can model Equation (8) by a linear system as

$$\mathrm{clp}(X_k[i]) = \alpha X_k[i] + \mathrm{clpn}(X_k[i]) \tag{9}$$

Here, $\alpha \equiv \mathrm{E}[X_k^*[i]\mathrm{clp}(X_k[i])]/\mathrm{E}[|X_k[i]|^2]$ is a constant where '$*$' denotes complex conjugate, and

$$\mathrm{clpn}(X_k[i]) \equiv \mathrm{clp}(X_k[i]) - \alpha X_k[i] \tag{10}$$

is the clipping noise which is statistically uncorrelated with $X_k[i]$. The above modelling will be used to design the detector in the next section.

For convenience, we will refer to $\boldsymbol{x}_k$ and $\boldsymbol{X}_k$ as the frequency- and time-domain transmit signal vectors, respectively. From the above discussions, we have

$$\boldsymbol{X}_k = \boldsymbol{F}\boldsymbol{x}_k, \quad \boldsymbol{x}_k = \left(\frac{1}{Q}\right)\boldsymbol{F}^H\boldsymbol{X}_k \tag{11}$$

where $\boldsymbol{F}$ is a $QN \times N$ matrix with (i, n)th entry given by $\mathrm{e}^{j\frac{2\pi in}{QN}}/\sqrt{N}$ and '$(\cdot)^H$' denotes conjugate transpose of matrix. (Note: Equation (11) can be computed using the fast Fourier transform technique.) The time-domain clipping noise vector is defined as

$$\mathrm{clpn}(\boldsymbol{X}_k) \equiv [\mathrm{clpn}(X_k[0]), \cdots, \mathrm{clpn}(X_k[QN-1])]^T \tag{12}$$

and its frequency-domain counterpart is given by

$$\boldsymbol{d}_k \equiv [d_k[0], \cdots, d_k[N-1]]^T = \left(\frac{1}{Q}\right)\boldsymbol{F}^H\mathrm{clpn}(\boldsymbol{X}_k) \tag{13}$$

For a complex random variable x with real part x^{Re} and imaginary part x^{Im}, we define its mean and variance as $\mathrm{E}[x] = \mathrm{E}[x^{\mathrm{Re}}] + j\mathrm{E}[x^{\mathrm{Im}}]$ and $\mathrm{Var}[x] = \mathrm{E}[|x|^2] - |\mathrm{E}[x]|^2$, respectively.

[†] Clipping incurs out-of-band radiation in an over-sampled OFDM system [6]. Band-pass filtering can mitigate this effect, but it may lead to PAPR re-growth. An iterative clipping and filtering process can be applied to resolve this problem [7].

4. RECEIVER PRINCIPLES

Assume perfect synchronisation. The core of the OFDM-IDMA receiver consists of an elementary signal estimator (ESE) and K *a posteriori* probability decoders (APP DECs). See Figure 2. The APP decoding is a standard function, so we will focus on the ESE.

After the OFDM demodulation, the frequency-domain received signal can be represented as

$$r[n] = \alpha \sum_{k=1}^{K} h_k[n]x_k[n] + \sum_{k=1}^{K} h_k[n]d_k[n] + z[n] \tag{14}$$

where $z[n]$ is a complex AWGN with variance N_0, $d_k[n]$ (defined in Equation (13)) represents the clipping noise from user k, and $h_k[n]$ is the channel coefficient related to the nth sub-carrier for user k. Note that $r[n]$ in Equation (14) is the signal after the OFDM demodulation. From the IDMA layer, the combination of the OFDM layer and physical channel can be viewed as a bank of N parallel sub-channels, each corresponding to an OFDM sub-carrier. With this view, ISI has already been resolved by the OFDM layer and we will focus on the MAI treatment in the IDMA layer.

Focusing on $x_k[n]$, we can rewrite Equation (14) as

$$r[n] = \alpha h_k[n]x_k[n] + \xi_k[n] \tag{15}$$

where

$$\xi_k[n] = \alpha \sum_{m=1, m\neq k}^{K} h_m[n]x_m[n] + \sum_{m=1}^{K} h_m[n]d_m[n] + z[n] \tag{16}$$

is the distortion component in $r[n]$ with respect to $x_k[n]$. From the central limit theorem, $\xi_k[n]$ can be approximated by a complex Gaussian random variable when K is large. (For simplicity, we assume that its real and imaginary parts have the same variance.) The statistics of $x_m[n]$ can be estimated from the DEC feedbacks [5]. Assume that $\mathrm{E}[d_m[n]]$ and $\mathrm{Var}[d_m[n]]$ are available. Then the iterative detection procedure in Reference [5] can be modified as follows:

(i) The ESE computes $\{\mathrm{E}[\xi_k[n]], \mathrm{Var}[\xi_k[n]]\}$ based on Equation (16) as

$$\mathrm{E}[\xi_k[n]] = \alpha \sum_{m=1, m\neq k}^{K} h_m[n]\mathrm{E}[x_m[n]] + \sum_{m=1}^{K} h_m[n]\mathrm{E}[d_m[n]]$$

Copyright © 2008 John Wiley & Sons, Ltd.

$$\mathrm{Var}[\xi_k[n]] = |\alpha|^2 \sum_{m=1, m\neq k}^{K} |h_m[n]|^2 \mathrm{Var}[x_m[n]] + \sum_{m=1}^{K} |h_m[n]|^2 \mathrm{Var}[d_m[n]] + N_0 \quad (17)$$

The *extrinsic* log-likelihood ratio (LLR) about $x_k^{\mathrm{Re}}[n]$ is given by

$$e_{\mathrm{ESE}}(x_k^{\mathrm{Re}}[n]) \equiv \ln\left(\frac{\Pr(r[n]|x_k^{\mathrm{Re}}[n]=+1)}{\Pr(r[n]|x_k^{\mathrm{Re}}[n]=-1)}\right) = \frac{4\,|\alpha h_k[n]|}{\mathrm{Var}\,[\xi_k[n]]}\mathrm{Re}(\mathrm{e}^{-j\theta_k[n]}(r[n]-\mathrm{E}[\xi_k[n]])) \quad (18)$$

where we have assumed $\alpha h_k[n] = |\alpha h_k[n]|\mathrm{e}^{j\theta_k[n]}$, and 'Re(·)' denotes the real part of a number. Similarly, we can compute $e_{\mathrm{ESE}}(x_k^{\mathrm{Im}}[n])$.

(ii) Taking the ESE outputs as inputs, the DECs perform APP decoding. The DEC feedbacks are then used to refine the means and variances of $x_k[n]$ and $d_k[n]$. Return to Step (i) for the next iteration.

5. TREATMENT OF CLIPPING NOISE

The remaining problem now is to find $\mathrm{E}[d_k[n]]$ and $\mathrm{Var}[d_k[n]]$. One way is simply ignoring them (i.e. setting them to zeros in Equation (17)) but this may incur considerable performance loss. A better way is estimating them iteratively as follows. From Equation (11), each entry X of $\boldsymbol{X}_k$ is a weighted sum of N random variables. When N is large, we can model X as a complex Gaussian random variable, that is $X \sim \mathcal{CN}(\mathrm{E}[X], \mathrm{Var}[X])$. The mean $\mathrm{E}[X]$ and variance $\mathrm{Var}[X]$ can be estimated from $\{\mathrm{E}[x_k[n]], \mathrm{Var}[x_k[n]]\}$. Let $p(X) = \mathrm{e}^{-|X-\mathrm{E}[X]|^2/\mathrm{Var}[X]}/(\pi \mathrm{Var}[X])$. Then

$$\mathrm{E}[\mathrm{clpn}(X)] = \int_{|X|\geqslant 0} \mathrm{clpn}(X)p(X)dX \quad (19a)$$

$$\mathrm{Var}[\mathrm{clpn}(X)] = \int_{|X|\geqslant 0} |\mathrm{clpn}(X)|^2 p(X)dX - |\mathrm{E}[\mathrm{clpn}(X)]|^2 \quad (19b)$$

In practice, Equation (19) can be evaluated using a look-up table [8]. With Equation (19), we have the following procedure for finding $\mathrm{E}[d_k[n]]$ and $\mathrm{Var}[d_k[n]]$.

(i) Generate $\{\mathrm{E}[X_k[i]], \mathrm{Var}[X_k[i]]\}$ (based on Equation (11) and $\{\mathrm{E}[x_k[n]], \mathrm{Var}[x_k[n]]\}$).
(ii) Find $\mathrm{E}[\mathrm{clpn}(X_k[i])]$ and $\mathrm{Var}[\mathrm{clpn}(X_k[i])]$ (based on a look-up table for Equation (19)).
(iii) Generate $\{\mathrm{E}[d_k[n]], \mathrm{Var}[d_k[n]]\}$ (based on Equation (13) and $\{\mathrm{E}[\mathrm{clpn}(X_k[i])], \mathrm{Var}[\mathrm{clpn}(X_k[i])]\}$).

In the first iteration, we may set $\mathrm{E}[d_k[n]]$ to zero and $\mathrm{Var}[d_k[n]]$ to its average without any *a priori* information.

6. PERFORMANCE ANALYSIS AND OPTIMISATION

We now outline an analysis technique for the above scheme. It is an extension of the SNR evolution technique for the plain IDMA [5] and is in spirit similar to the *extrinsic* information transfer (EXIT) char technique, except that SNR is used instead of mutual information. The main purpose is to provide a faster and more convincing assessment means without time-consuming simulation. Two additional issues for OFDM-IDMA are frequency-selective fading and clipping noise. We will develop analysis techniques for these two types of distortion. We will also demonstrate the application of the fast analysis technique in searching-based system design so as to achieve the MUG discussed in Section 2.

6.1. Performance prediction

Assume that $\{h_k[n], \forall k, \forall n\}$ are mutually independent. (This assumption follows the fully interleaved fading modelling in Reference [4], which is approximately true if interleaver length is sufficiently long.) According to the discussions in Section 4, user-k's signal is detected by treating $\xi_k[n]$ in Equation (15) as a Gaussian noise with mean $\mathrm{E}[\xi_k[n]]$ and variance $\mathrm{Var}[\xi_k[n]]$. Denote by I_k the average of $\mathrm{Var}[\xi_k[n]]$ over index n. From Equation (17),

$$I_k \equiv \mathrm{E}[\mathrm{Var}[\xi_k[n]]] = \sum_{m=1, m\neq k}^{K} \eta_m(|\alpha|^2 v_{x,m} + v_{d,m}) + \eta_k v_{d,k} + N_0 \quad (20)$$

where $\eta_m \equiv \mathrm{E}[|h_m[n]|^2]$ is user-m's average channel gain, while $v_{x,m} \equiv \mathrm{E}[\mathrm{Var}[x_m[n]]]$ and $v_{d,m} \equiv \mathrm{E}[\mathrm{Var}[d_m[n]]]$ are the average variances of the signal and clipping noise from user m, respectively. We will approximate all

Copyright © 2008 John Wiley & Sons, Ltd.

$\mathrm{Var}[\xi_k[n]]$, $\forall n$, by their average, that is

$$\mathrm{Var}[\xi_k[n]] \approx I_k, \quad n = 0, 1, \cdots, N-1. \tag{21}$$

This approximation greatly simplifies the problem. From Equations (15) and (18), we have

$$\begin{aligned} &\mathrm{e}_{\mathrm{ESE}}(x_k^{\mathrm{Re}}[n]) + j\mathrm{e}_{\mathrm{ESE}}(x_k^{\mathrm{Im}}[n]) \\ &\approx \frac{4\,|\alpha h_k[n]|}{I_k}(|\alpha h_k[n]| x_k[n] + \mathrm{e}^{-j\theta_k[n]}(\xi_k[n] - \mathrm{E}[\xi_k[n]])) \end{aligned} \tag{22}$$

Then, the performance of the ESE can be approximately characterised by the SNR with respect to $x_k[n]$ in Equation (22), that is

$$\gamma_k \equiv \frac{\mathrm{E}[|\alpha h_k[n] x_k[n]|^2]}{\mathrm{E}[|\xi_k[n] - \mathrm{E}[\xi_k[n]]|^2]} = \frac{2|\alpha|^2 \eta_k}{I_k} \tag{23}$$

where we have assumed that all users have the same transmit power $\mathrm{E}[|x_k[n]|^2] = 2$. The average variance $v_{x,m}$ in Equation (20) characterises the uncertainty in user-m's signal after the APP decoding. Thus, its value depends fully on the DEC inputs and the FEC code employed. The case for the average variance $v_{d,m}$ of the clipping noise is similar, but it is also related to the clipping parameters. Given the coding/clipping schemes, $v_{x,m}$ and $v_{d,m}$ can be characterised by the following two functions:

$$v_{x,m} = f(\gamma_m), \quad v_{d,m} = c(\gamma_m) \tag{24}$$

Similarly, we can characterise the relationship between BER and γ_m by a function as

$$\mathrm{BER}_m = g(\gamma_m) \tag{25}$$

The three functions in Equations (24) and (25) can be pre-simulated by applying the Monte-Carlo method to a single-user system. Notice that $f(\cdot)$ and $g(\cdot)$ in Equations (24) and (25) are similar to the two tables defined by Equations (16) and (17) in Reference [5]. However, there is a subtle difference. In Reference [5], the two tables can be generated by pre-simulation in an AWGN channel. Here the underlying OFDM layer is modelled by a bank of parallel channels with individual fading coefficients. (See Equation (14).) The channel for pre-simulation should be modelled accordingly. Assume that these tables are available. Let It be the total number of iterations. Denote by $\gamma_k^{(q)}$ the value of γ_k after q iterations. The SNR evolution procedure is listed below:

(i) Initialisation: Set $\gamma_k^{(0)} = 0$, $k = 1, 2, \cdots, K$.
(ii) SNR updating: For $q = 0, 1, \cdots, It-1$, compute

$$\gamma_k^{(q+1)} = \frac{2|\alpha|^2 \eta_k}{\sum_{m=1, m\neq k}^{K} \eta_m \left(|\alpha|^2 f\left(\gamma_m^{(q)}\right) + c\left(\gamma_m^{(q)}\right)\right) + \eta_k c\left(\gamma_k^{(q)}\right) + N_0}, \quad k = 1, 2, \cdots, K \tag{26}$$

Termination: Find the BER by substituting the final values of $\{\gamma_k\}$ into Equation (25).

The effectiveness of this technique will be demonstrated by the numerical examples in Section 8.

6.2. *MUG and power allocation*

The information-theoretical analysis of MUG in Section 2 is for capacity-achieving codes and optimal detection. For practical OFDM-IDMA schemes, rigorous theoretical analysis of MUG is difficult due to the sub-optimality of the FEC, the frequency selectiveness of the channel and the nonlinear nature of the iterative receiver. However, the underlying rationale in achieving MUG suggests that it can be realised by practical OFDM-IDMA with proper design.

As shown in Section 2, the MUG is achieved by ordered matching the sets of received signal power and channel gain. We therefore consider a two-step strategy which first optimises the received power profile and then applies ordered matching to allocate the transmit power. The SNR evolution technique can be used as the underlying tool to accelerate the search of received power profile. We will omit the details because the principle is very similar to that discussed in Reference [5]. The results presented in Section 8 are all based on this strategy.

7. SPREADING AND SUPERPOSITION CODING

OFDM-IDMA can work with any FEC coding. However, low-rate coding is particularly attractive because it can provide more robust performance in frequency-selective channels. An even simpler approach is to introduce spreading after FEC coding, which is similar to OFDM-CDMA [4].‡ With spreading, each bit is 'spread' as 'chips' over different OFDM sub-carriers. At the receiver, the

‡ The purpose of spreading in OFDM-IDMA is purely for diversity gain rather than user separation as in OFDM-CDMA [4]. OFDM-IDMA relies on chip-level, user-specific interleaving to distinguish users.

Copyright © 2008 John Wiley & Sons, Ltd.

DOI: 10.1002/ett

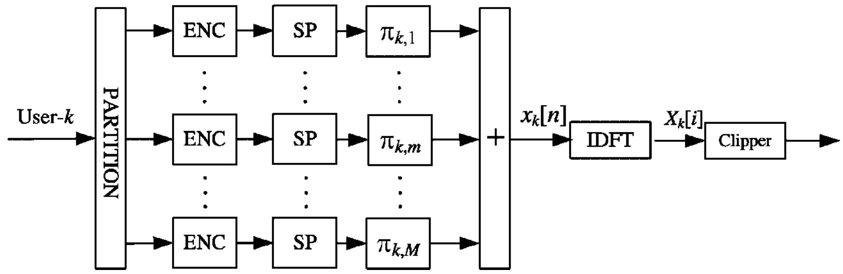

Figure 3. Transmitter structure of OFDM-IDMA with superposition coding, where SP represents spreader.

information is collected from these sub-carriers. This results in diversity that averages out the fading effect.

Spreading reduces throughput but this can be compensated by superposition coding [8]. With superposition coding, each user can transmit more than one coded sequence using a multi-layer encoder, as shown in Figure 3. In this way, high-rate transmission and very flexible rate adjustment can be achieved. For example, different number of layers can be assigned to different users according to their channel conditions. The receiver principle is similar to that in Section 4 (since a layer in Figure 3 is equivalent to a user in Figure 2) and the details are omitted here. Later we will show that given the transmission rates of the users, the introduction of spreading and superposition coding can yield noticeable performance improvement.

Receiver complexity increases when more layers are involved. This is mainly due to the ESE cost that increases linearly with the spreading length. The cost related to despreading is marginal and the cost related to DEC, which usually dominates the receiver complexity, is independent of spreading. Overall, the cost increase is quite moderate.

The above superposition coding scheme has an additional advantage regarding the clipping issue that it is more robust to clipping effect than other alternatives such as bit-interleaved coded modulation with iterative decoding (BICM-ID) [10]. This interesting property of superposition coding is briefly explained below. Recall that the clipping noise estimation in Section 5 is based on $\{E[x_k[n]], \mathrm{Var}[x_k[n]]\}$ that are computed from the *extrinsic* LLRs about the coded bits of the DECs. Denote by v_k the average of $\mathrm{Var}[x_k[n]]$ over n. Generally speaking, a smaller v_k implies a more accurate estimate of $x_k[n]$, which in turn implies a more accurate estimate of clipping noise. (In the extreme case of $v_k = 0$, the estimates of all $\{x_k[n]\}$ are perfect. Then the estimates of their IDFT $\{X_k[i]\}$ are also perfect and so are the clipping noise estimates computed from Equation (19).) Clearly, v_k can be used to characterise the accuracy in estimating $x_k[n]$. We find that v_k is significantly affected by the coding scheme

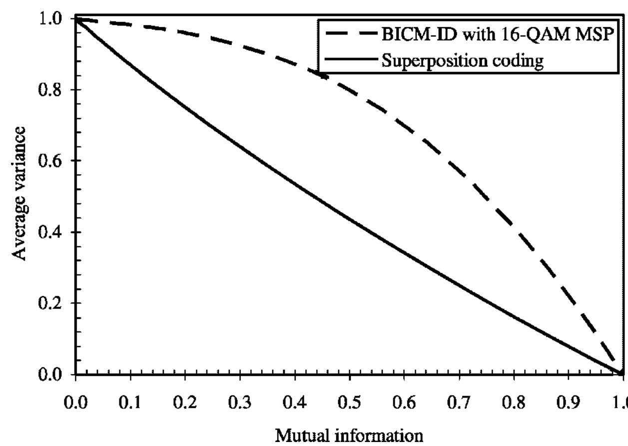

Figure 4. Average variance achieved by different coding schemes. The average power of $x_k[n]$ is normalised to 1.

employed. Furthermore, it can be proved that superposition coding achieves the minimum v_k among all possible coding schemes (for the same DEC feedbacks). We omit the related proof as it is beyond the scope of this paper. Instead, we provide in Figure 4 a comparison between a two-layer superposition coding scheme and a BICM-ID scheme with 16-QAM modified set-partitioning (MSP) signaling [10]. The rates of both schemes are the same. The *extrinsic* LLRs of the DECs are assumed to be i.i.d. Gaussian and characterised by the mutual information between them and the coded bits. From Figure 4, superposition coding yields smaller average variance, implying that it may outperform BICM-ID in mitigating clipping effect. This is one of the reasons for the advantage (in addition to MUG) of OFDM-IDMA presented in Figure 7.

8. NUMERICAL RESULTS AND DISCUSSIONS

We set the number of sub-carriers to $N = 256$, the oversampling factor $Q = 4$ and the clipping ratio $\mathrm{CR} = 0\,\mathrm{dB}$. With the clipping and filtering technique, the PAPR of

Copyright © 2008 John Wiley & Sons, Ltd.

DOI: 10.1002/ett

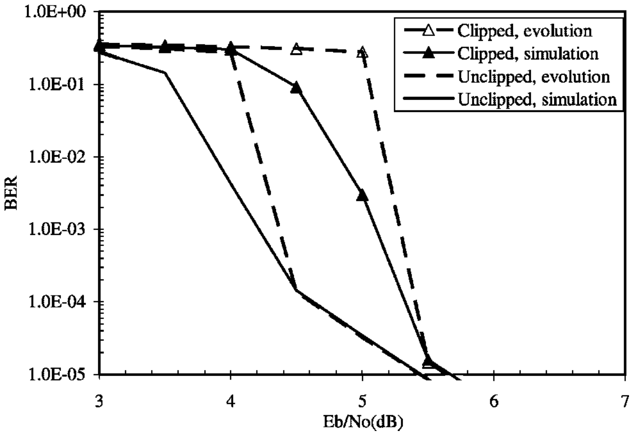

Figure 5. Performance of OFDM-IDMA with and without clipping. The spreading length is $S = 8$. The rate of each user is 1/8. $K = 16$. $R = 2$. The information block length for each user is 512. All users have the same transmit power.

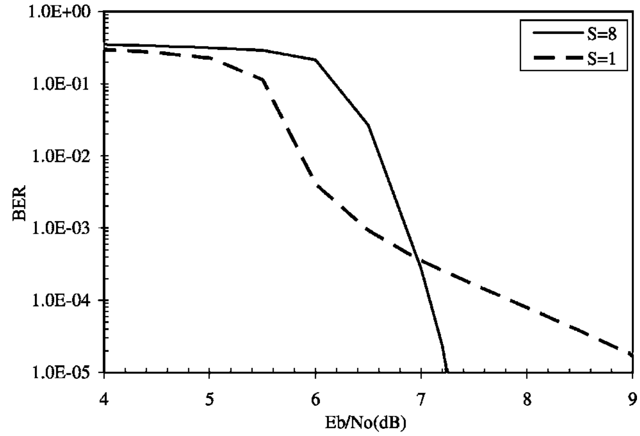

Figure 6. Performance comparison of different two-user OFDM-IDMA schemes. The information block lengths for each layer are 4096 and 512, respectively, for $S = 1$ and 8 so that the interleaver lengths are the same. All layers have the same transmit power.

the transmit signal can be reduced to less than 5.9 dB for 99.9 per cent of the OFDM blocks, in contrast to 11.3 dB in the unclipped case. For simplicity, the overhead due to cyclic prefixing is ignored below. Unless otherwise stated, we assume a fully interleaved Rayleigh fading channel [4], where $\{h_k[n]\}$ are i.i.d. complex-Gaussian with mean 0 and variance 1. The rate-1/2 convolutional code $(23, 35)_8$ is always used for the ENC. The number of iterations is 10.

We first examine the efficiency of the SNR evolution technique. Figure 5 shows the performance of a 16-user OFDM-IDMA system. (The parameters are listed in the caption.) It is seen that the evolution and simulation results agree with each other. It is also seen that the iterative detector outlined in Section 4 can efficiently recover the performance loss due to clipping.

We next show the performance of OFDM-IDMA schemes with superposition coding. Let $K = 2$ and rate per user = 1 bit/s/Hz. Two different spreading lengths, that is, $S = 1$ and $S = 8$, are considered. In order to support the required transmission rate, the layer numbers for each user are set to 1 and 8 for $S = 1$ and 8, respectively. Figure 6 demonstrates that the scheme with $S = 8$ significantly outperforms that with $S = 1$ in achieving a low BER (e.g. 10^{-5}). This confirms the advantage of spreading and superposition coding in OFDM-IDMA systems.

Figure 7 demonstrates the impact of MUG as discussed in Section 2. We assume that the transmitters have knowledge of the path loss and log-normal fading factors (the same as those in Figure 1) but have no knowledge of the Rayleigh fading coefficients. We set $S = 8$ and consider a sum rate $R = 3$, so a total of 24 layers are involved. We consider different numbers of users. For simplicity, we assume that all users employ the same number of layers. Thus, each user has one layer when $K = 24$, and two layers when $K = 12$, and so on. The linear-programming method [5] is used for optimising the received power profile and the results are listed in Table 1. The ordered matching in Equations (3) and (5) is applied to the received power profile in Table 1 to determine the transmit power profile. For comparison, we consider OFDMA using a rate-3 BICM-ID scheme with the 16-QAM MSP signaling [10]. Interleaved sub-carrier allocation [11] is assumed for OFDMA. Clipping is also applied to OFDMA to reduce the PAPR and an iterative

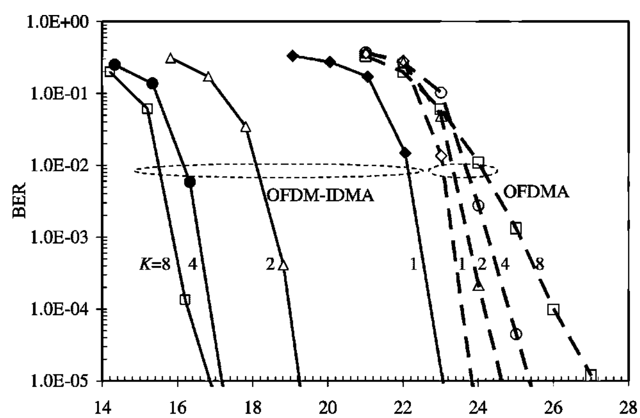

Figure 7. Comparison of the power efficiency of OFDM-IDMA and OFDMA with clipping in an uplink scenario. The over-sampling factor $Q = 4$ and clipping ratio CR = 0 dB. $R = 3$. The power of the channel noise is set to 1 (i.e. 0 dB).

Copyright © 2008 John Wiley & Sons, Ltd.

DOI: 10.1002/ett

Table 1. Received power profile of the OFDM-IDMA systems in Figure 7.

Layer number	12	5	5	2
Power level (dB)	0	3.1673	5.5427	6.3345

detector similar to that discussed in Section 4 is applied to combat the clipping effect. The same latency is assumed for the OFDM-IDMA and OFDMA schemes. Thus, the block length of OFDMA decreases as K increases. We can show that the two schemes have comparable complexities.

From Figure 7, OFDM-IDMA outperforms OFDMA, especially for a large K. When $K = 4$, OFDM-IDMA can achieve about 8 dB gain compared with OFDMA. There are several reasons for this. First, the non-orthogonal OFDM-IDMA scheme can realise the MUG. Second, OFDM-IDMA with spreading can achieve significant diversity gains. Third, BICM-ID-based OFDMA is more sensitive to the clipping effect than OFDM-IDMA. (See Section 7.) Finally, BICM-ID performance degrades when block length reduces.

9. CONCLUSIONS

We have outlined an SNR evolution technique for performance prediction and optimisation for OFDM-IDMA. We have shown that OFDM-IDMA can (i) alleviate the PAPR problem commonly suffered by OFDM-based schemes; (ii) deliver significant MUG compared with other orthogonal alternatives; (iii) provide robust communication in frequency-selective channels; and (iv) support high single-user throughput.

ACKNOWLEDGEMENT

This work was supported by a grant from the Research Grant Council of the Hong Kong SAR, under Project CityU 116706.

REFERENCES

1. Mahafeno I, Langlais C, Jego C. OFDM-IDMA versus IDMA with ISI cancellation for quasi-static Rayleigh fading multipath channels. In *Proceedings of the 4th International Symposium on Turbo Codes and Related Topics*, Munich, Germany, 3–7 April 2006.
2. Schoeneich H, Hoeher PA. Adaptive interleave-division multiple access-a potential air interference for 4G bearer services and wireless LANs. In *Proceedings of 1st IEEE and IFIP International Conference on Wireless and Optical Communications and Networks (WOCN 2004)*, Muscat, Oman, June 2004, pp. 179–182.
3. Li P, Guo Q, Tong J. The OFDM-IDMA approach to wireless communication systems. *IEEE Wireless Communications Magazine* 2007; **14**(3):18–24.
4. Fazel K, Kaiser S. *Multi-Carrier and Spread Spectrum Systems.* John Wiley Sons: Chichester, UK, 2003.
5. Liu LH, Tong J, Li P. Analysis and optimization of CDMA systems with chip-level interleavers. *IEEE Journal on Selected Areas in Communications* 2006; **24**(1):141–150.
6. Li X, Cimini LJ. Effects of clipping and filtering on the performance of OFDM. *IEEE Communication Letters* 1998; **2**(5):131–133.
7. Armstrong J. Peak-to-average power reduction for OFDM by repeated clipping and frequency domain filtering. *Electronic Letters* 2002; **38**(5):246–247.
8. Tong J, Li P, Ma X. Superposition coded modulation with peak-power limitation. *IEEE Transactions on Information Theory*, in press.
9. Tse D, Viswanath P. *Fundamentals of Wireless Communication*. Cambridge University Press: Cambridge, 2005.
10. Tan J, Stuber GL. Analysis and design of symbol mappers for iteratively decoded BICM. *IEEE Transactions on Wireless Communications* 2005; **4**(2):662–672.
11. Hou SW, Ko CH. Multiple-access interference supression for interleaved OFDM system uplink. *IEEE Transactions on Vehicular Technology* 2008; **57**(1):194–205.

Copyright © 2008 John Wiley & Sons, Ltd.